

Monitoring Macromolecular Motions on Microsecond to Millisecond Time Scales by $R_{1\rho}$ – R_1 Constant Relaxation Time NMR Spectroscopy

Mikael Akke and Arthur G. Palmer, III*

Department of Biochemistry and Molecular Biophysics
Columbia University, 630 West 168th Street
New York, New York 10032

Received October 18, 1995

Dynamic processes on microsecond to millisecond (μ s–ms) time scales are important for the functions of proteins, including recognition, allostery, and catalysis.^{1,2} Intramolecular motions on μ s–ms time scales contribute to nuclear magnetic relaxation through adiabatic dephasing of coherent states and are exhibited as conformational exchange phenomena in solution-state NMR spectroscopy.³ Nuclear magnetic relaxation in the rotating frame (i.e., in the presence of a radiofrequency (rf) field) constitutes a unique source of information on chemical and conformational exchange processes.⁴ This communication presents a new rotating frame technique for studying intra- and intermolecular exchange in proteins^{5–8} that overcomes several difficulties associated with existing spin-lock and spin-echo experiments. First, rotating frame and laboratory frame relaxation rate constants are averaged during a novel constant relaxation time (CRT) period in order to simplify the off-resonance effects normally encountered in spin-lock experiments. Second, an off-resonance spin-lock rf field^{9–11} is used to increase the magnitude of the effective magnetic field in the rotating frame in order to access faster dynamic processes. The off-resonance $R_{1\rho}$ – R_1 CRT nuclear magnetic relaxation experiment allows determination of conformational exchange times at least as short as 25 μ s in proteins.

The effect of conformational (or chemical) exchange on the off-resonance rotating frame relaxation rate constant, $R_{1\rho}^{\text{off}}$, is described by⁸

$$R_{1\rho}^{\text{off}} = R_1 \cos^2 \theta + R_2 \sin^2 \theta + R_{\text{ex}} \sin^2 \theta \quad (1)$$

in which $\theta = \arctan(\omega_1/\Delta\omega)$ is the “tilt angle” between the directions of the reduced static field, $\Delta\omega = \omega - \omega_0$, and the effective field, $\omega_e = (\omega_1^2 + \Delta\omega^2)^{1/2}$, in the rotating frame; ω is the spin-lock rf frequency; ω_1 is the spin-lock field strength in units of rad/s; ω_0 is the population-averaged chemical shift; R_1 and R_2 are the spin–lattice and spin–spin relaxation rate constants, respectively; and R_{ex} is the contribution to the transverse relaxation rate from exchange processes. For exchange between two sites A and B,⁸

$$R_{\text{ex}} = (\delta\omega)^2 p_A p_B \tau_{\text{ex}} / (1 + \tau_{\text{ex}}^2 \omega_e^2) \quad (2)$$

in which p_i is the population of spins in site i , $\delta\omega = \omega_A - \omega_B$ is the chemical shift difference between the two sites, and $\tau_{\text{ex}} = 1/k_{\text{ex}} = p_B/k_{A \rightarrow B} = p_A/k_{B \rightarrow A}$ is the time constant for the exchange process. The off-resonance spin-lock experiment allows ω_e to be varied by changing ω while keeping ω_1 constant in order to minimize sample heating effects. In addition, complications that arise because the resonance frequencies for the (two) individual conformations (e.g., ω_A and ω_B) differ from ω_0 are mitigated because $\Delta\omega \gg \delta\omega$. The desired exchange parameters, $(\delta\omega)^2 p_A p_B$ and τ_{ex} , cannot be determined in practice simply by measuring $R_{1\rho}^{\text{off}}$ as a function of ω_e , because $\cos^2 \theta \rightarrow 1$ and $\sin^2 \theta \rightarrow 0$ as ω is shifted off-resonance.

The pulse sequence for the off-resonance $R_{1\rho}$ – R_1 CRT experiment is illustrated in Figure 1. Following an initial refocused INEPT^{12,13} polarization transfer from I (^1H) to S (^{15}N) spins (point a), the S spin coherence is aligned along the direction of the effective field of the off-resonance spin lock (point b). After a spin-locking period of length t (point c), the S spin coherence is returned to the z -axis (point d) for a laboratory frame relaxation period $T - t$, in which T is the total CRT period (point e). Finally, the S spin coherence is returned to the transverse plane, frequency-labeled during t_1 , and transferred back to the I spins for detection. The signal intensity is given by¹⁴

$$\begin{aligned} I(t) &= I_0 \exp[-R_{1\rho}^{\text{off}} t] \exp[-R_1(T - t)] \\ &= I_0 \exp[-R_1 T] \exp[-(R_{1\rho}^{\text{off}} - R_1)t] \\ &= \tilde{I}_0 \exp[-R_{\text{eff}} t] \end{aligned} \quad (3)$$

in which $\tilde{I}_0 = I_0 \exp[-R_1 T]$ is the signal intensity at $t = 0$, I_0 is a constant, and

$$R_{\text{eff}} = R_{1\rho}^{\text{off}} - R_1 = (R_2 - R_1 + R_{\text{ex}}) \sin^2 \theta \quad (4)$$

Equation 4 can be recast using eq 2 as

$$R_{\text{eff}}/\sin^2 \theta = R_2 - R_1 + (\delta\omega)^2 p_A p_B \tau_{\text{ex}} / (1 + \tau_{\text{ex}}^2 \omega_e^2) \quad (5)$$

The resonance offset dependence is reduced to a scaling factor $\sin^2 \theta$ that is determined solely by the known parameters ω , ω_1 , and ω_0 . The number of free parameters is also reduced compared with eqs 1 and 2, because R_2 and R_1 appear only as the difference $R_2 - R_1$. Experimentally, R_{eff} is measured as a function of ω_e by varying ω , and the parameters $(\delta\omega)^2 p_A p_B$, τ_{ex} , and $R_2 - R_1$ are determined by nonlinear curve-fitting to eq 5.

The off-resonance $R_{1\rho}$ – R_1 CRT experiment is demonstrated for a 1 mM uniformly ^{15}N -labeled sample of the fibronectin type III domain of the extracellular matrix protein tenascin ($M_r = 10.1$ kDa).^{15,16} Representative relaxation curves for the backbone amide ^{15}N spin of residues D30 ($\delta = 118.81$ ppm), R45 ($\delta = 123.11$ ppm), and N55 ($\delta = 120.35$ ppm) are shown in Figure 2. Values for $R_{\text{eff}}/\sin^2 \theta$ determined at eight effective field strengths are shown in Figure 3. For maximum precision, $R_2 - R_1$ were fixed at values calculated from laboratory frame R_1 and NOE measurements (P. A. Carr and A. G. Palmer, unpublished results) using the model free formalism of Lipari and Szabo¹⁷ and a rotational correlation time of 4.4 ns. The

(1) Fersht, A. *Enzyme Structure and Mechanism*, 2nd ed.; W. H. Freeman & Co.: New York, 1985; pp 1–475.

(2) Creighton, T. E. *Proteins. Structures and Molecular Properties*, 2nd ed.; W. H. Freeman & Co.: New York, 1993; pp 1–507.

(3) Wennerström, H. *Mol. Phys.* **1972**, *24*, 69–80.

(4) Deverell, C.; Morgan, R. E.; Strange, J. H. *Mol. Phys.* **1970**, *18*, 553–559.

(5) Szyperski, T.; Luginbühl, P.; Otting, G.; Güntert, P.; Wüthrich, K. *J. Biomol. NMR* **1993**, *3*, 151–164.

(6) Orekhov, V. Y.; Pervushin, K. V.; Arseniev, A. S. *Eur. J. Biochem.* **1994**, *219*, 887–896.

(7) Tjandra, N.; Kuboniwa, H.; Ren, H.; Bax, A. *Eur. J. Biochem.* **1995**, *230*, 1014–1024.

(8) Davis, D. G.; Perlman, M. E.; London, R. E. *J. Magn. Reson., Ser. B* **1994**, *104*, 266–275.

(9) Jones, G. P. *Phys. Rev.* **1966**, *148*, 332–335.

(10) Jacquinot, J. F.; Goldman, M. *Phys. Rev. B* **1973**, *8*, 1944–1957.

(11) James, T. L.; Matson, G. B.; Kuntz, I. D.; Fisher, R. W. *J. Magn. Reson.* **1977**, *28*, 417–426.

(12) Morris, G. A.; Freeman, R. *J. Am. Chem. Soc.* **1979**, *101*, 760–762.

(13) Burum, D. P.; Ernst, R. R. *J. Magn. Reson.* **1980**, *39*, 163–168.

(14) Mandel, A. M.; Palmer, A. G. *J. Magn. Reson., Ser. A* **1994**, *110*, 62–72.

(15) Erickson, H. P.; Bourdon, M. A. *Annu. Rev. Cell Biol.* **1989**, *5*, 71–92.

(16) Leahy, D.; Hendrickson, W. A.; Aukhil, I.; Erickson, H. P. *Science* **1992**, *258*, 987–991.

(17) Lipari, G.; Szabo, A. *J. Am. Chem. Soc.* **1982**, *104*, 4546–4559.

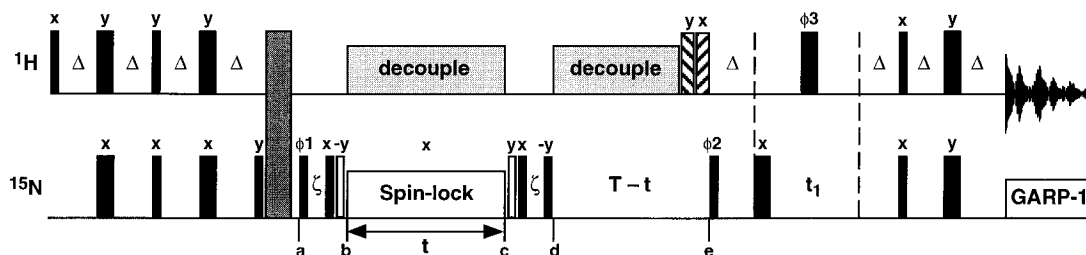


Figure 1. Pulse sequence for the off-resonance $R_{1\rho}$ - R_1 CRT experiment. The narrow and wide solid bars depict 90° and 180° pulses, respectively. The narrow empty bars depict pulses with a flip angle $90^\circ - \arctan(\omega_1/\Delta\omega_c)$. High-power pulses are applied with a field strength ω_{1c} and with the transmitter frequency ω_c centered in the ^{15}N spectrum. The wide gray bar depicts a homospoil gradient pulse. The wide hatched bars depict high-power purge pulses of 0.5–1.0 ms duration. ^1H decoupling is applied during the relaxation delays using the WALTZ-16 sequence¹⁸ or a train of ^1H 180° pulses. ^{15}N decoupling during acquisition is performed using GARP-1.¹⁹ The off-resonance spin-lock field is applied as continuous irradiation with a constant field strength ω_1 and offset $\Delta\omega_c = \omega - \omega_c$. The frequency is switched phase-coherently from ω_c to ω at point b and switched back at point c. The elements between a and b and between c and d serve to rotate the coherences between the z-axis and the directions of effective field for the ^{15}N spins. Numerical solutions of the Bloch equations indicate that the delay $\zeta = \omega_1/(\delta\omega_c^2 + \omega_1^2) - 2/\omega_{1c}$ is optimal for $\omega_{1c} \gg |\omega_0 - \omega_c|$; $\zeta = 0$ is satisfactory when this formula yields a negative value, provided that $\omega_1 \geq |\omega_0 - \omega_c|$. The first term of ζ is determined by the contribution to θ due to chemical shift offset,^{20,21} and the second term compensates for evolution during pulses.^{22,23} The phase cycle is $\phi_1 = y, -y$; $\phi_2 = y, y, -y, -y, y, y, -y, -y$; $\phi_3 = 4(x), 4(-x)$; receiver = $x, -x, -x, x, -x, x, x, -x$. Quadrature detection in the indirect dimension uses the States-TPPI phase cycling scheme.²⁴ The sequence can be elaborated to include sensitivity enhancement,²⁵ gradient coherence selection,²⁶ or coherence transfer using cross polarization.²⁷

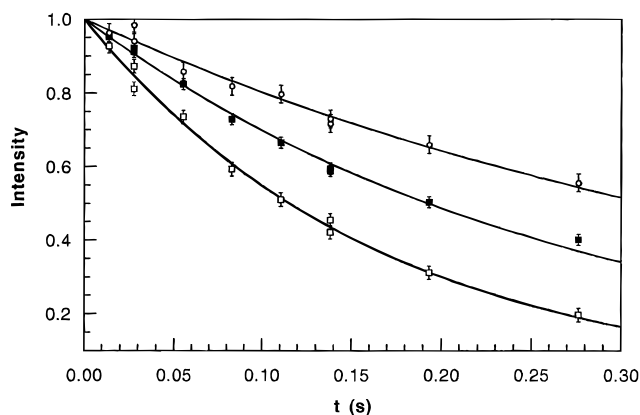


Figure 2. Representative relaxation curves for the ^{15}N off-resonance CRT $R_{1\rho}$ - R_1 experiment obtained using a spin-lock field strength of 2330 ± 30 Hz and an offset of 46 ppm from the center of the ^{15}N spectrum. Residue D30 (\circ , $\theta = 45.1^\circ$), R45 (\blacksquare , $\theta = 42.9^\circ$), and N55 (\square , $\theta = 44.2^\circ$). The decay was monitored using eight spin-lock periods, two of which were obtained in duplicate in order to assess the peak intensity error.

optimized values of τ_{ex} and $(\delta\omega)^2 p_{\text{APB}}$ are D30, $88 \pm 68 \mu\text{s}$ and $(61 \pm 24) \times 10^3 \text{ s}^{-2}$; R45, $46 \pm 5 \mu\text{s}$ and $(2.15 \pm 0.05) \times 10^5 \text{ s}^{-2}$; and N55, $27 \pm 2 \mu\text{s}$ and $(4.5 \pm 0.2) \times 10^5 \text{ s}^{-2}$. Assuming equally populated conformers ($p_A = p_B = 0.5$), $\delta\omega = 492 \pm 308 \text{ s}^{-1}$ (1.5 ± 1.0 ppm), $927 \pm 141 \text{ s}^{-1}$ (2.9 ± 0.4 ppm), and $1342 \pm 264 \text{ s}^{-1}$ (4.2 ± 0.8 ppm) for D30, R45, and N55, respectively. For comparison, if $R_2 - R_1$ is treated as a free parameter, the optimized values of τ_{ex} and $(\delta\omega)^2 p_{\text{APB}}$ are

(18) Shaka, A. J.; Keeler, J.; Frenkiel, T.; Freeman, R. *J. Magn. Reson.* **1983**, *52*, 334–338.

(19) Shaka, A. J.; Barker, P. B.; Freeman, R. *J. Magn. Reson.* **1985**, *64*, 547–552.

(20) Griesinger, C.; Ernst, R. R. *J. Magn. Reson.* **1987**, *75*, 261–271.

(21) Yamazaki, T.; Muhandiram, R.; Kay, L. E. *J. Am. Chem. Soc.* **1994**, *116*, 8266–8278.

(22) Cavanagh, J.; Fairbrother, W. J.; Palmer, A. G.; Skelton, N. J. *Protein NMR Spectroscopy: principles and practice*; Academic Press: San Diego, 1995; pp 1–587.

(23) Bax, A.; Marion, D. *J. Magn. Reson.* **1988**, *78*, 186–191.

(24) Marion, D.; Ikura, M.; Tschudin, R.; Bax, A. *J. Magn. Reson.* **1989**, *85*, 393–399.

(25) Palmer, A. G.; Cavanagh, J.; Wright, P. E.; Rance, M. *J. Magn. Reson.* **1991**, *93*, 151–170.

(26) Kay, L. E.; Keifer, P.; Saarinen, T. *J. Am. Chem. Soc.* **1992**, *114*, 10663–10665.

(27) Krishnan, V. V.; Rance, M. *J. Magn. Reson., Ser. A* **1995**, *116*, 97–106.

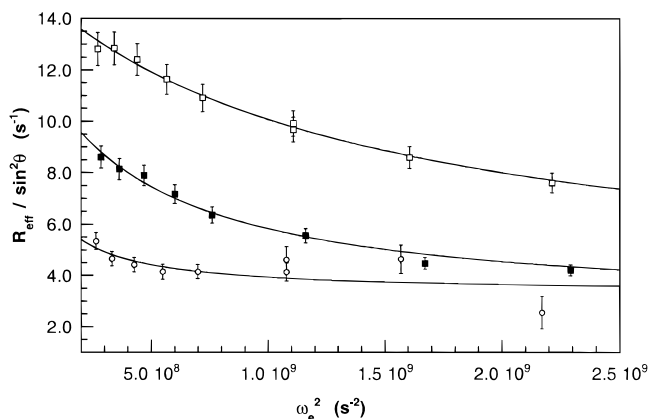


Figure 3. Curve fits of eq 5 to the experimental $R_{\text{eff}}/\sin^2 \theta$ data for residues D30 (\circ), R45 (\blacksquare), and N55 (\square) obtained at eight different effective fields. The spin-lock field strength was 2330 ± 30 Hz. The offsets from the center of the ^{15}N spectrum were 138, 115, 92, 69, 57, 46, 34, and 23 ppm (corresponding to nominal tilt angles of 18.4, 21.8, 26.6, 33.7, 38.7, 45.0, 53.1, and 63.4°). A duplicate data set was acquired for an offset of 92 ppm.

R45, $35 \pm 9 \mu\text{s}$ and $(2.8 \pm 0.8) \times 10^5 \text{ s}^{-2}$; N55, $24 \pm 9 \mu\text{s}$ and $(5.5 \pm 3.7) \times 10^5$; data for D30 could not be fit reliably.

In conclusion, the off-resonance $R_{1\rho}$ - R_1 CRT relaxation experiment offers significant advantages for characterizing exchange processes on μs – ms time scales in complex biological macromolecules: (i) the dynamics of multiple sites in a complex molecule can be investigated in a single experiment, (ii) only moderate spin-lock field strengths are required, and (iii) differences between the effective fields experienced by a nuclear spin in different conformations are minimized.

Acknowledgment. We thank Drs. V. V. Krishnan, Ann McDermott, and Mark Rance for many helpful discussions. ^{15}N -Labeled tenascin fibronectin type III domain was a generous gift from Gina Briscoe and Harold P. Erickson (Duke University). We thank Peter A. Carr (Columbia University) for providing laboratory frame relaxation data on tenascin. M.A. gratefully acknowledges a postdoctoral fellowship from the Swedish Natural Sciences Research Council and a travel grant from the Swedish Medical Sciences Research Council. This work was supported by grants from the Arnold and Mabel Beckmann Foundation, the NIH (GM50291), and the NSF (MCB9419049), awarded to A.G.P.